



# Investigating the $|S_{11}|$ Parameter of CPW-Fed Antennas for WiMAX and WLAN Applications

Anupam Kr. Yadav<sup>1,2</sup> · Suman Lata<sup>1</sup> · Sandeep Kr. Singh<sup>1</sup> · Arvind Kr. Singh<sup>3</sup> · Tripurari Sharan<sup>3</sup> · M. Z. A. Yahya<sup>4</sup>

Received: 8 October 2022 / Accepted: 6 March 2023 / Published online: 4 April 2023  
© The Minerals, Metals & Materials Society 2023

## Abstract

This communication presents a novel, low-profile coplanar waveguide (CPW)-fed dual-band microstrip antenna for wireless applications. The proposed antenna consists of an inverted L-shaped slot radiator coupled with a U-shaped ground plane and two vertical ground terminals. It is implemented on FR4-epoxy dielectric substrate material ( $\epsilon_r = 4.4$ ,  $\tan \delta = 0.02$ ) with dimensions of  $56 \times 56 \text{ mm}^2$  and generates two desired resonant frequencies at about 2.40 GHz and 3.48 GHz for WLAN and WiMAX applications, respectively. The antenna shows two distinct bands, first from 2.34 to 2.54 (200 MHz at  $-20 \text{ dB}$ ) and second from 3.25 to 3.60 (350 MHz at  $-12 \text{ dB}$ ), which cover the entire WLAN ( $f_c = 2.4 \text{ GHz}$ , 2.400–2.484 GHz) and WiMAX ( $f_c = 3.5 \text{ GHz}$ , 3.400–3.690 GHz) bands. This work aims to combine WLAN and WiMAX communication standards simultaneously into a single device by designing a single antenna that can excite dual-band operation. Also, numerical findings are presented for the antenna's return loss and 2D radiation patterns. Good agreement between measured and simulated outcomes is established. The results indicate that the proposed antenna, which performs well, may be appropriate for WLAN/WiMAX applications, including those involving portable electronics and emerging technologies.

**Keywords** CPW · WiMAX · WLAN ·  $S_{11}$ -parameter

## Introduction

Wireless local-area networks (WLAN) and Worldwide Interoperability for Microwave Access (WiMAX) are commonly used by mobile devices such as handheld computers and smartphones to access the Internet. The WLAN/WiMAX modules which are utilized to access these environments are able to function over a number of frequency bands. The most common options for these devices are microstrip patch antennas because of their appealing properties, including

easy feeding, low profile, affordable production, and ease of integration. The WLAN and WiMAX frequencies specified by the Federal Communications Commission (FCC) are respectively centered at 2.4 GHz, 5.2 GHz, and 5.8 GHz and 2.5 GHz, 3.5 GHz, and 5.5 GHz. For WLAN/WiMAX applications, a variety of microstrip antennas with various shapes have been experimentally studied to minimize size and increase bandwidth.<sup>1–4</sup> Coplanar waveguide (CPW)-fed wide slot antennas have received much attention and are being increasingly used because of the advantages of wide bandwidth, low profile, planar geometry, and easy integration with monolithic microwave integrated circuits and stable radiation patterns.<sup>5–7</sup>

A nonuniform meander-line and a fork-type ground were proposed for triple-band WLAN applications by Wu et al.<sup>8</sup> To enhance the bandwidth, a dual-wideband monopole antenna was realized with a parasitic patch using an electromagnetic coupling mechanism to cover the entire WLAN and WiMAX bands.<sup>9</sup> An asymmetric M-shaped patch was used to design a triple-band antenna, and vias on the long arm of the patch are used for the purpose of compactness.<sup>10</sup> A compact wideband monopole antenna with

✉ Sandeep Kr. Singh  
hit.ssk@gmail.com

<sup>1</sup> Department of Electrical Electronics and Communication Engineering, SET, Sharda University, Greater Noida, India

<sup>2</sup> Department of Electronics and Communication Engineering, SET, Noida International University, Greater Noida, India

<sup>3</sup> North Eastern Regional Institute of Science and Technology, Nirjuli, Arunachal Pradesh, India

<sup>4</sup> Faculty of Defence Science and Technology, Universiti Pertahanan Nasional Malaysia, Kuala Lumpur, Malaysia

enough bandwidth to cover the WLAN operating bands was obtained by Huang and Yu.<sup>11</sup> A CPW-fed printed monopole antenna with an n-shaped slot for dual-band operation was presented by Fan et al.<sup>12</sup> An asymmetric coplanar strip (ACS)-fed structure was introduced by Li et al.<sup>13</sup>

For dual-, triple-, and quad-band applications, CPW-fed patch antenna designs with various structural form have been proposed. As reported in previous works,<sup>14–16</sup> slot-loading techniques have been used to minimize the size of a patch antenna and create multiband functioning within a certain frequency range. Size reduction and impedance matching are accomplished using substrate material and slot approaches for numerous communication systems, as reported by Singh et al.<sup>17</sup> Therefore, several microstrip antenna designs for both WLAN and WiMAX applications have been proposed in order to develop an antenna that covers multiband and broadband operations. Most of these designs, like CPW-fed patch monopole and defected ground structure (DGS) antenna approaches, are based on slot antennas and fed by a CPW.<sup>18</sup>

In this work, a simple configuration of a CPW-fed dual-band microstrip antenna is proposed to cover the operational bands of WLAN and WiMAX. The proposed antenna consists of an inverted L-shaped slot radiator coupled with a U-shaped ground plane and two vertical ground terminals of the same thickness that are etched on a square patch to achieve dual-band operation. The design and analysis are performed using the CST MICROWAVE STUDIO full-wave electromagnetic simulator. In order to validate the technical proposal, the optimized antenna is realized and measured. The proposed antenna with a compact size of  $56 \times 56 \text{ mm}^2$  generates two desired resonant frequencies at around 2.40 GHz (2.34–2.54 GHz) and 3.48 GHz (3.25–3.60 GHz), and provides good omnidirectional radiation patterns. The measured and simulated return loss of the antenna is presented.

The details of the antenna design and the simulated results are presented and discussed in the following sections. The dimensions and evolution process of the proposed antenna are introduced in the "Introduction" section. In the "Antenna Geometry and Design Steps" section, a parametric study is carried out to determine the effects of the different parameters of the antenna and to obtain an optimal design structure. The results of the measurement are given in the "Parametric Study of the Proposed Antenna" section, and then the conclusion is presented in the "Results and Discussion" section.

## Antenna Geometry and Design Steps

### Antenna Geometry

The shape of the proposed CPW-fed square patch antenna is depicted in Fig. 1d, with geometrical design parameters. The proposed antenna (step-4) was designed on an FR4 substrate with a thickness of 0.76 mm, dielectric constant ( $\epsilon_r$ ) = 4.3, loss tangent ( $\tan\delta$ ) of 0.017, and overall dimensions of  $56 (L) \times 56 (W) \text{ mm}^2$ . An inverted L-shaped radiator stub and square ring ground plane with a thickness of 0.08 mm are implanted on the upper layer of the substrate. The outer dimensions of the square ring are  $56 \times 56 \text{ mm}^2$  and the inner dimensions are  $40 \times 40 \text{ mm}^2$ , with a U-shaped ground plane and two vertical ground terminals. The radiating patch is made of an inverted L-shaped stub with a thickness of 5.7 mm and lengths  $L_x$  and  $L_y$  of 30 mm in both directions with  $50 \Omega$  impedance.

### Design Steps

Figure 1a, b, c and d illustrates the evolution of several prototypes of the antenna which have been developed and

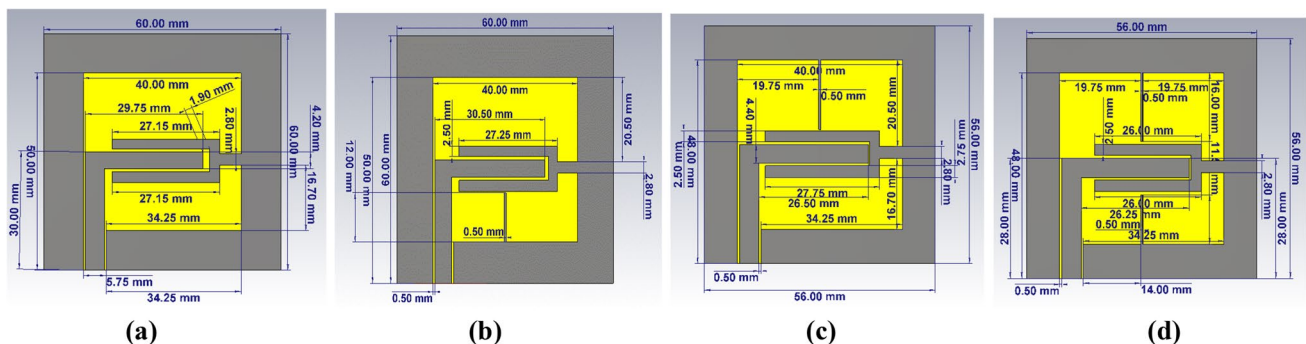


**Fig. 1** Design steps of the CPW-fed broadband square slot antennas. (a) Design step-1: antenna-1, inverted L-shaped CPW-fed-line coupled with U-shaped ground terminal. (b) Design step-2: antenna-2, simplified step-1 structure with straight-line lower-ground tuning

stub. (c) Design step-3: antenna-3, simplified step-2 structure with straight-line upper-ground tuning stub. (d) Proposed design step-4: Proposed antenna-4, modified with both lower and upper ground terminals.

investigated. The antenna design in step-1 simply used an inverted L-shaped CPW-fed line coupled with a U-shaped ground terminal, shown in Fig. 1a. The step-2 design used a simplified structure of step 1 with a vertical straight-line lower-ground terminal tuning stub, as shown in Fig. 1b, and in the step-3 design, the author merely simplified the antenna-2 structure with a vertical straight-line upper-ground terminal tuning stub, shown in Fig. 1c. In step-4, the author adapted the antenna-2 and antenna-3 structures with both lower- and upper-ground terminals, shown in Fig. 1d. The simulated results of the impedance bandwidth (IBW) and return loss ( $S_{11}$ -parameter) demonstrated in Fig. 2a, b, c and d reveal that the wideband performance is controlled by four-resonant-mode geometry.

The antenna design steps are investigated for dual-band applications with various geometrical configurations as shown in Fig. 1a, b, c and d. The obtained results show that the first resonant frequency ( $fr_1$ ) is approximately fixed at 3.5 GHz, and the second resonant frequency ( $fr_2$ ) is shifted towards the lower-frequency range near 2.5–1.8 GHz, as displayed in Fig. 3. The optimal values ( $|S_{11}|$ ) of several prototypes of the antenna are listed in Table I.

## Parametric Study of the Proposed Antenna

To obtain optimal antenna performance, parametric research is important for understanding how each parameter affects the outcomes of the antenna. This study, during which just one parameter is varied and the others are fixed, is based on antenna design step-1 to step-4. The effects of the antenna size on the impedance bandwidth and the frequency range of the antenna are explored using a variety of factors.

### Performance of $|S_{11}|$ Parameter

The length of ground terminal stub resonators is widely considered during the design of the antenna to achieve the number of resonant frequencies and bands of CPW-fed antennas. Resonant frequencies and bands can be controlled by changing the length of the ground terminal stubs according to the user requirements.<sup>18</sup> The parametric study is based on an inverted L-shaped radiating stub coupled with a symmetrical U-shaped ground plane and two vertical ground terminals.

The effects of the resonant path length (inverted-L length in x-direction,  $L_x$ ) on the return loss  $|S_{11}|$  of antenna-1 (step-1) are displayed in Fig. 4. The length of the stub ( $L_x$ ) varies from 25 mm to 30 mm. The fundamental resonant frequency ( $fr_1$ ) is approximately 3.5 GHz for the entire range from 26 mm to 29.75 mm for the single-band operation. The variation in the  $|S_{11}|$  parameter of antenna-1 for step-1 is illustrated in Fig. 4.

The effects of the resonant path length (lower vertical ground terminal,  $L_{LT}$ ) on the return loss  $|S_{11}|$  of antenna-2 (step-2) are presented in Fig. 5. The stub length is varied with the help of the lower vertical ground terminal ( $L_{LT}$ ). The  $L_{LT}$  is changed as 9.50 mm to  $\leq L_{LT} \leq 11.50$  mm. The stability of magnitude of  $|S_{11}|$  increases as the length of  $L_{LT}$  is increased. The two resonant frequencies are found for dual-band application as  $fr_1 = 3.4$  GHz and  $fr_2 = 1.8$  GHz for the first and second bands operation. The variation in the return loss of the step-2 antenna is displayed in Fig. 5. The length of the lower vertical ground terminal stub is optimized at  $L_{LT} = 9.5$  mm, 10.0 mm, 10.5 mm, 11.0 mm, and 11.5 mm, with fixed inverted-L stub length.

The length of the upper vertical ground terminal ( $L_{UT}$ ) stub is varied to analyze the characteristics of antenna-3 (step-3). The stub length used to enhance the  $|S_{11}|$  characteristics with the ground stub  $L_{UT}$  variation ( $14.50$  mm  $\leq (L_{UT}) \leq 16$  mm) are presented in Fig. 6. A significant change in resonant frequencies  $fr_1$  (1.3 GHz),  $fr_2$  (2.15 GHz), and  $fr_3$  (3.6 GHz) occurs for the first, second, and third bands. The Opti-1 result proves that  $L_{UT} = 16$  mm produces wide IBW with a maximum magnitude of  $|S_{11}|$  and fixed inverted-L stub length ( $L_x$ ).

The optimal length of the U-shaped arms ( $U_{XA}$ ) stub with two vertical ground terminals, namely lower ( $L_{LT}$ ) and upper ( $L_{UT}$ ), can be used for the best  $|S_{11}|$  characteristics of the proposed antenna (step-4). The variation in the length of plane ground stub  $U_{XA}$  in the range of  $23$  mm  $\leq U_{XA} \leq 26$  mm, with a fixed length of vertical ground terminals ( $L_{LT}/L_{UT}$ ) and ( $L_x$ ), used to improve the  $|S_{11}|$  characteristic is presented in Fig. 7. In the step-4 design, the first resonant frequency ( $fr_1$ ) is fixed at 3.5 GHz and the second resonant frequency ( $fr_2$ ) is shifted to lower bands ranging from 2.4 GHz to 2.25 GHz according to optimization (From Opti-1 to Opti-5) of the length of  $U_{XA}$ . When the length of stub  $U_{XA}$  is taken as 26 mm, the antenna produces appropriate resonant frequencies  $fr_1$  and  $fr_2$  which are close to each other at 2.5 GHz ( $-27$  dB) and 3.5 GHz ( $-38$  dB) for WiMAX bands, as displayed in the Opti-1 result in Fig. 7.

## Results and Discussion

### Return Loss

The performance and results of the proposed antenna-4 were measured with the CST EM Studio version 17 simulator and vector network analyzer (N5224B). The parametric analysis of the antenna, which is expected for WLAN and WiMAX broadband antennas, is carried out and presented in Fig. 8(a, b). Simulated and measured results (return loss,  $S_{11} \leq -10$  dB) of antenna-4 are in reasonable agreement,

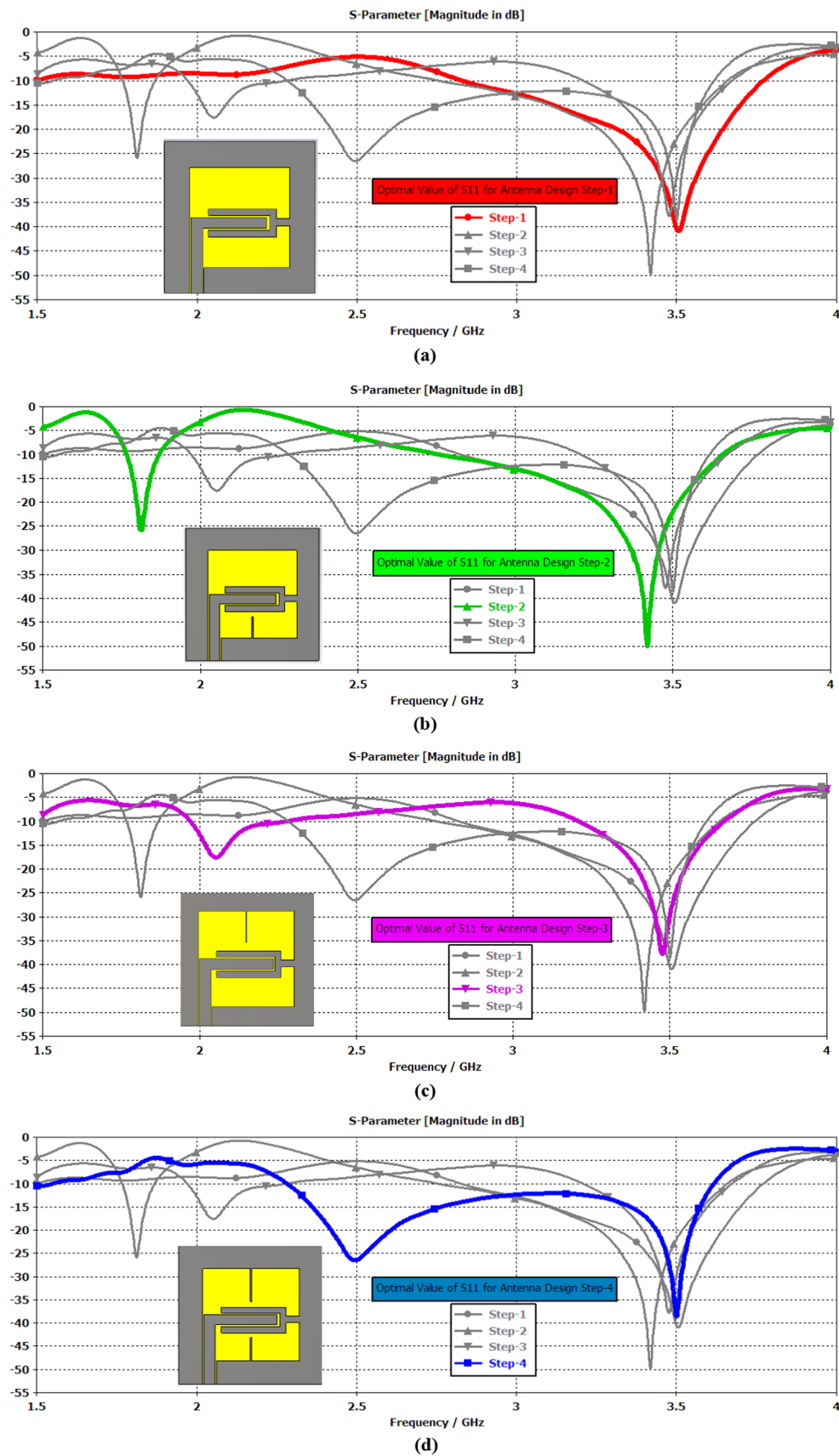


**Fig. 2** Optimal values of  $|S_{11}|$  parameter for all design steps: (a) step-1, (b) step-2 (c) step-3, and (d) step-4.

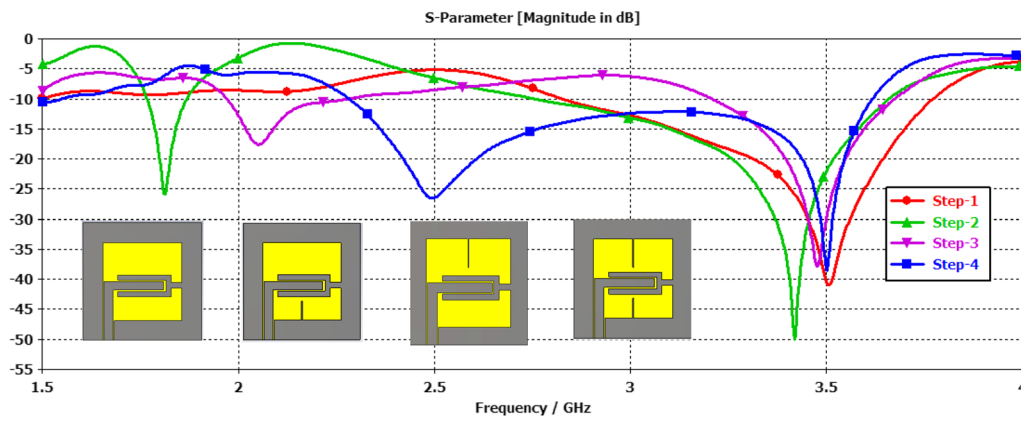


Fig. 3 Comparison of  $|S_{11}|$  parameter from design step-1 to step-4.

Table I Best electrical performance  $|S_{11}|$  comparison of the design antennas

Antenna design steps	Resonant frequency ( $f_r$ ) and impedance bandwidth (IBW)				
	$f_{r1}$ (GHz)	IBW <sub>1</sub> ( $S_{11} \leq -10$ dB) (GHz, -dB)	$f_{r2}$ (GHz)	IBW <sub>2</sub> ( $S_{11} \leq -10$ dB) (GHz, -dB)	Bands
Step-1	3.50	2.80–3.75, 10	–	–	Single
Step-2	3.40	2.75–3.65, 10	1.80	1.75–1.85, 10	Dual
Step-3	3.48	3.20–3.65, 10	2.05	1.95–2.20, 10	Dual
Step-4	3.50	3.35–3.60, 15	2.50	2.35–2.75, 15	Dual

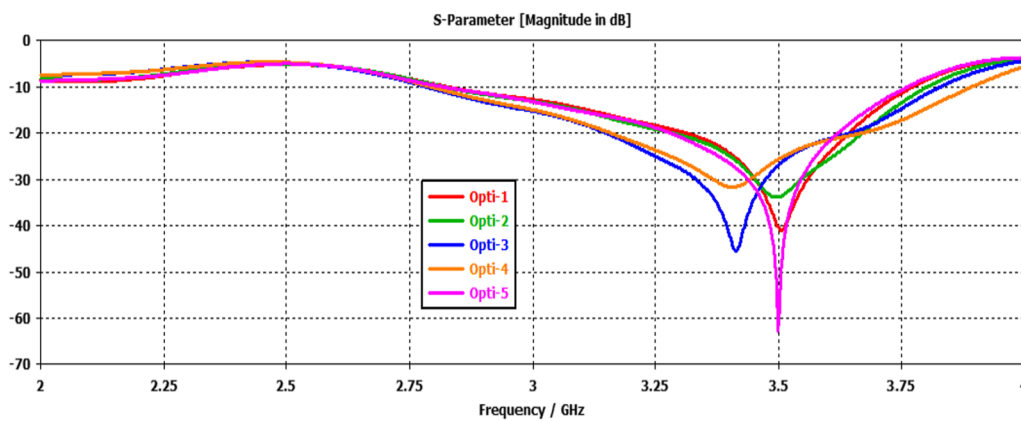


Fig. 4  $|S_{11}|$  performance of antenna design step-1 under development investigation.

and the best value of IBW can reach 47.46% (1.40 GHz, 2.25–3.65 GHz), as displayed in Fig. 8a and b.

The measured return loss of antenna-4 ensures a dual-band operation as shown in Fig. 8b, which indicates resonant frequency ( $f_{r1}$ ) of 3.5 GHz with  $-28$  dB return loss and an impedance bandwidth of 350 MHz (3.25–3.60 GHz) at  $-15$  dB. The second resonant frequency ( $f_{r2}$ ) is 2.4 GHz with  $-58$  dB return loss and an impedance bandwidth of 200 MHz (2.34–2.54 GHz). Thus, the proposed antenna-4 shows the desired dual-band characteristics, and these are WLAN and WiMAX bands (Table II).

### Radiation Pattern

The radiation pattern of an antenna is a graphical representation of the radiation properties of the antenna. The simulated E-plane and H-plane radiation patterns of the CPW-fed antenna-4 with two resonant frequencies of 2.5 and 3.5 GHz are presented in Fig. 9.

Figure 9a and b depicts far-field co-polarization patterns in the E-plane ( $\phi = 0^\circ$ ) and H-plane ( $\phi = 90^\circ$ ), respectively at 2.5 GHz. It can be seen that the antenna has bidirectional co-polarized patterns for the WLAN

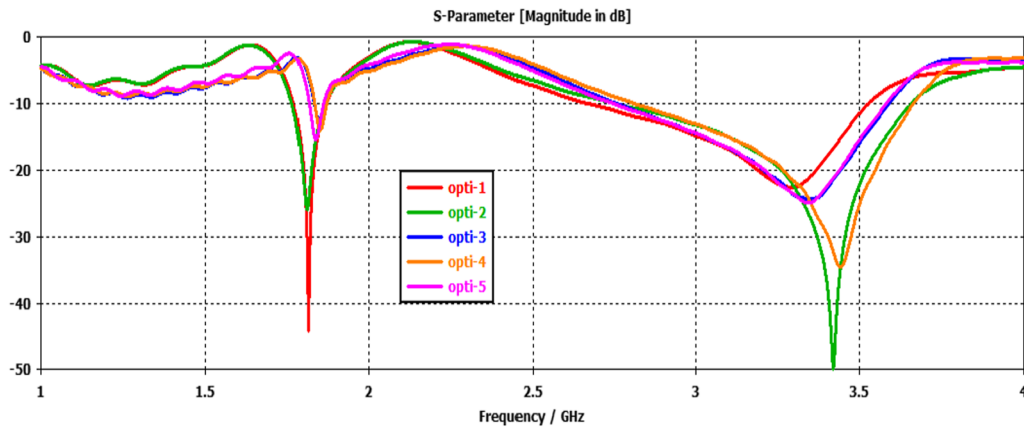


Fig. 5  $|S_{11}|$  performance of antenna design step-2 under development investigation.

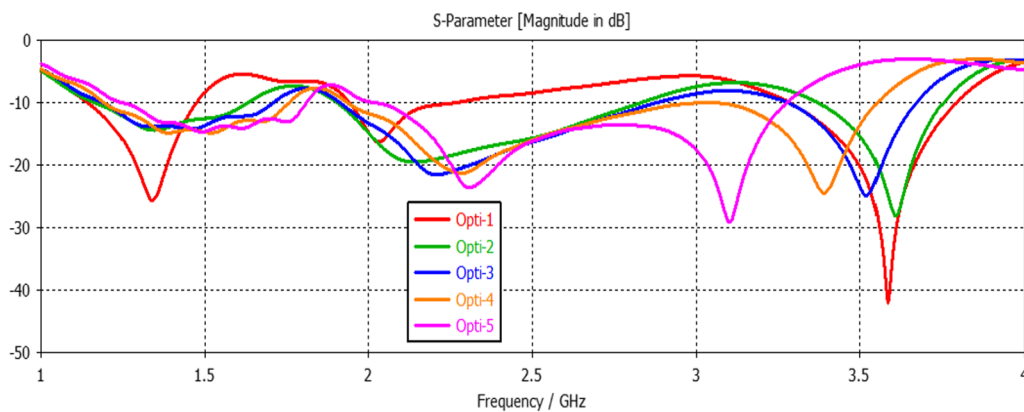


Fig. 6  $|S_{11}|$  performance of antenna design step-3 under development investigation.

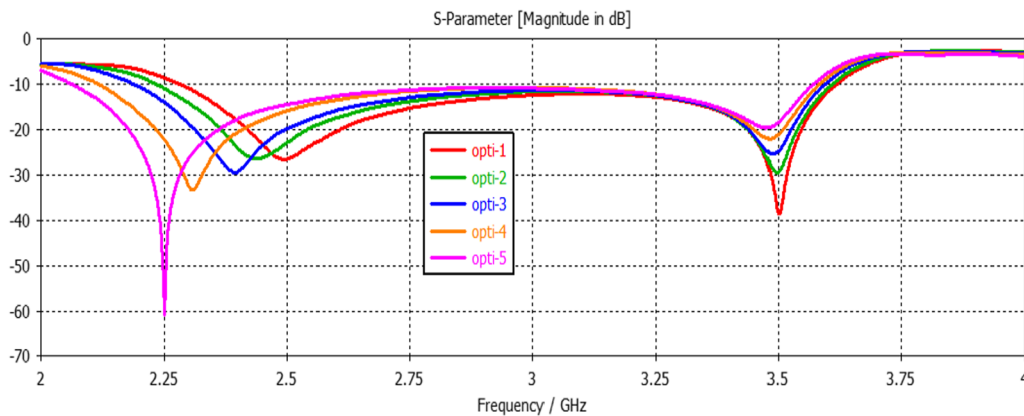


Fig. 7  $|S_{11}|$  performance of antenna design step-4 under development investigation.

band. Figure 9c and d illustrates that the co-polarization patterns of antenna-4 are fairly improved at 3.5 GHz as compared to 2.5 GHz in the E-plane and H-plane, respectively. At 3.5 GHz frequency, the proposed antenna-4

has omnidirectional radiation patterns in both the E- and H-plane for the WiMAX band.

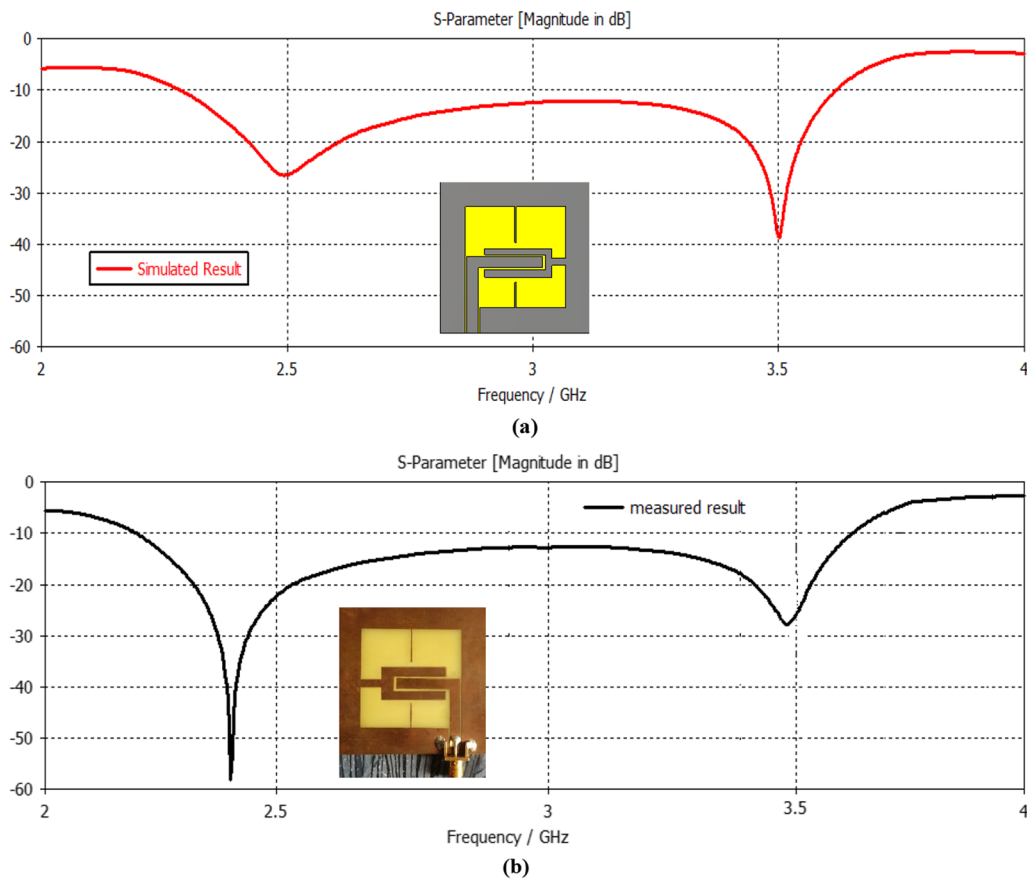


Fig. 8 Simulated and measured return loss of proposed antenna: (a) simulated, (b) measured.

Table II Performance comparison of simulated and measured data of proposed antenna-4

Results	$f_r$ (GHz)	$S_{11}$ (-dB)	IBW (GHz) at -dB	Gain (dB)
Simulation (CST)	3.5	38	3.35–3.60, -15 dB	4
	2.5	27	2.35–2.75, -15 dB	2
Measurement	3.5	28	3.25–3.60, -15 dB	–
	2.4	58	2.34–2.54, -20 dB	–

**Current Density**

To better understand the antenna performance, the surface current density of the dual-band proposed antenna-4 at frequency of 2.5 GHz and 3.5 GHz is simulated and illustrated in Fig. 10a and b, respectively. In Fig. 9a, the current density at 2.4 GHz is observed along with lower and upper vertical ground terminals and the near-to-gap area between the inverted L-shaped radiating patch and ground plane.

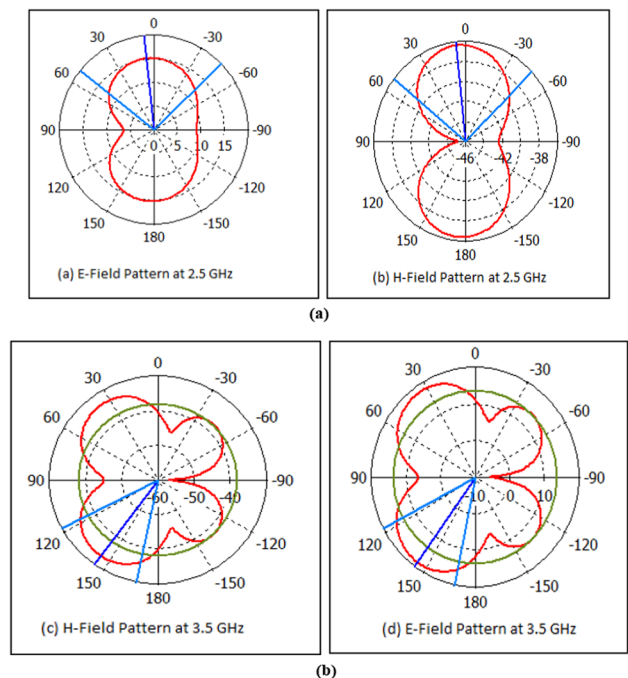


Fig. 9 Radiation patterns of proposed antenna: (a) 2.5 GHz and (b) 3.5 GHz.

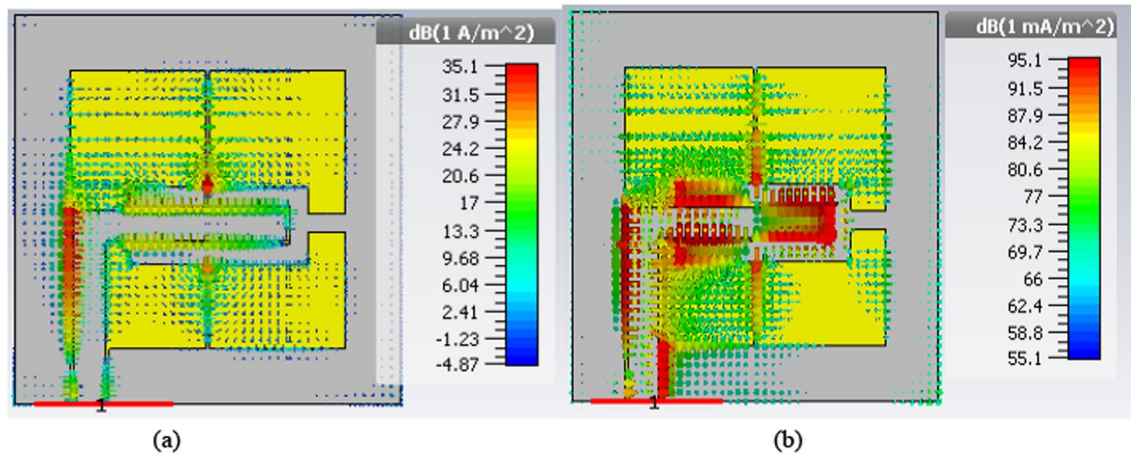


Fig. 10 Current density of proposed antenna at 2.5 GHz and 3.5 GHz.

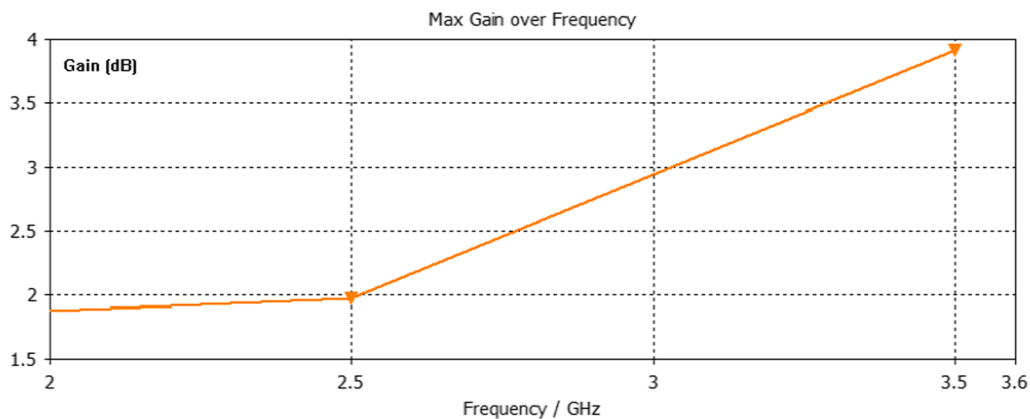


Fig. 11 Gain of proposed antenna at 2.5 GHz and 3.5 GHz.

Similarly, it can be seen from Fig. 10b that at current density of 3.5 GHz, a large surface current density is observed along the L-shaped radiating patch.

## Gain

The gain of the antenna is equal to the directivity of the antenna times its efficiency. The gain represents the focusing power of the antenna including its losses. Although the directivity of an antenna is often reported, very often its maximum gain is quoted. Figure 11 shows the maximum gain of antenna-4, which is approximately 2.0 dB at 2.5 GHz and 4.0 dB at 3.5 GHz.

Table III compares the performance of the final optimized antenna with previously reported antennas<sup>8–16</sup> fabricated on the same dielectric substrate (FR4,  $\epsilon_r = 4.4$ ,  $\tan \delta = 0.02$ ) for a fair comparison. Although the size of the proposed

antenna-4 is approximately the same as those previously reported,<sup>9,10,12,15</sup> the IBW is higher.

## Conclusions

The proposed novel dual-band CPW-fed antenna suitable for compact wireless communication devices in WLAN and WiMAX standards has been successfully simulated. This antenna is fabricated using FR4 substrate with dimensions of  $56 \times 56 \times 0.76 \text{ mm}^3$ . It has a simple structure and is easy to fabricate due to its planar structure. Moreover, the simulated and measured results confirm that the antenna is able to cover two bands of operation. The experimental results confirm that this antenna has two bands at 2.34–2.54 GHz and 3.25–3.60 GHz and two resonant frequencies at 2.4 GHz and 3.48 GHz, which cover the WLAN band (2.4 GHz) and WiMAX band (3.5 GHz), respectively; hence it effectively



**Table III** Performance comparison of the proposed antennas with other reported antennas

[Refs.] Year	Substrate material		Size (mm <sup>2</sup> )	Resonant frequency (GHz)			Oper- ating bands
	$(\epsilon_r)$	t (mm)		$f_{r(n)}$ : ( $n = 1, 2, 3$ )	$f_{r1}$	$f_{r2}$	
[8] 2006	FR4 (4.4)	0.80	120 × 40	2.45	5.45	–	2
[9] 2007	FR4 (4.4)	0.80	50 × 50	2.50	3.50	5.50	3
[10] 2010	Rogers (2.2)	2.00	64 × 62	2.44	3.55	–	3
[11] 2011	FR4 (4.4)	1.60	60 × 70	2.45	5.50	–	2
[12] 2012	FR4 (4.4)	1.60	50 × 25	2.00	2.45	–	2
[13] 2013	FR4 (4.4)	1.60	50 × 90	2.50	3.50	5.50	3
[14] 2018	FR4 (4.2)	1.60	70 × 70	2.31	2.40	2.48	3
[15] 2020	FR4 (4.4)	0.80	50 × 50	2.50	3.60	6.00	3
[16] 2021	FR4 (4.4)	1.60	116 × 116	1.02	1.75	–	2
Proposed antenna-4	FR4 (4.3)	0.76	56 × 56	2.40	3.50	–	2

integrates both standards with a single miniature device. This antenna provides gain of 2.0 dB and 4.0 dB at 2.5 GHz and 3.5 GHz, respectively. In addition, the proposed antenna achieves omnidirectional radiation patterns in the E/H-plane at 3.5 GHz and bidirectional in the E/H-plane at 2.5 GHz.

**Acknowledgments** The authors would like to acknowledge and convey their sincere thanks to the Center for Solar Cells and Renewable Energy, Sharda University, Greater Noida, India, for their valuable support.

**Conflict of interest** The authors declare that they have no conflict of interest regarding this study.

## References

1. T.L. Zhang, Z.H. Yan, L. Chen, and Y. Song, A compact dual-band CPW-fed planar monopole antenna for WLAN applications. *J. Electromagn. Waves Appl.* 22, 2097–2104 (2008).
2. W.C. Liua, C.M. Wua, and N.C. Chub, A compact low-profile dual-band antenna for WLAN and WAVE applications. *Int. J. Electron. Commun. (AEÜ)* 66, 467–471 (2012).
3. A. Kunwar, A.K. Gautam, and B.K. Kanaujia, “Inverted L-slot triple band antenna with defected ground structure for WLAN and WiMAX applications. *Int. J. Microw. Wirel. Technol.* (2016). <https://doi.org/10.1017/S1759078715001105>.
4. K.G. Jangid, P.K. Jain, B.R. Sharma, V.K. Saxena, V.S. Kulhar, and D. Bhatnagar, Ring slotted circularly polarized U-shaped printed monopole antenna for various wireless applications. *Adv. Electromagn.* 6(1), 70–76 (2017).
5. S. Jo, H. Choi, J. Lim, B. Shin, S. Oh, J. Lee, A CPW-fed monopole antenna with double rectangular rings and vertical slots in the ground plane for WLAN/WiMAX applications. *Int. J. Antennas Propag.* 2015, 2–9 (2015).
6. S.K. Singh, T. Sharan, and A.K. Singh, Characterization of broadband antenna based on FR-4 substrate material. *Mater. Today Proc.* 12(3), 628–635 (2019).
7. S.K. Singh, T. Sharan, and A.K. Singh, Enhancing the axial ratio bandwidth of circularly polarized open ground slot CPW-Fed antenna for multiband wireless communications. *Eng. Sci.* 17, 274–284 (2021).
8. C.M. Wu, C.N. Chiu, and C.-K. Hsu, A new non-uniform meandered and fork-type grounded antenna for triple-band WLAN applications. *IEEE Antennas Wirel. Propag. Lett.* 5(1), 346–349 (2006).
9. C.Y. Pan, T.S. Horng, W.S. Chen, and C.H. Huang, Dual wide-band printed monopole antenna for WLAN/WiMAX applications. *IEEE Antennas Wirel. Propag. Lett.* 6, 149–151 (2007).
10. L. Peng, C.L. Ruan, and X.H. Wu, Design and operation of dual/triple band asymmetric M-shaped microstrip patch antennas. *IEEE Trans. Antennas Propag.* 9, 1069–1072 (2010).
11. C.Y. Huang and E.Z. Yu, A slot-monopole antenna for dual-band WLAN applications. *IEEE Antennas Wirel. Propag. Lett.* 10, 500–502 (2011).
12. S.T. Fan, Y.Z. Yin, W. Hu, K. Song, and B. Li, Novel CPW-fed printed monopole antenna with an n-shaped slot for dual-band operations. *Microw. Opt. Technol. Lett.* 54(1), 240–242 (2012).
13. X. Li, X.-W. Shi, W. Hu, P. Fei, and J.F. Yu, Compact triband ACS-fed monopole antenna employing open-ended slots for wireless communication. *IEEE Trans. Antennas Propag.* 12, 388–391 (2013).
14. T. Dabas, B.K. Kanaujia, D. Gangwar, A.K. Gautam, and K. Rambabu, Design of multiband multi-polarised single feed patch antenna. *IET Microw. Antennas Propag.* 12, 2372–2378 (2018).
15. A.E. Yassini, S. Ibnyaich, S. Chabaa, and A. Zeroual, Miniaturized broadband multiband planar antenna with a symmetric quarter circular ground plane for WLAN/WiMAX standards. *Microw. Opt. Technol. Lett.* 10, 1–12 (2020).

16. R. Ma and Q. Feng, Design of broadband circularly polarized square slot antenna for UHF RFID applications. *Prog. Electromagn. Res. C* 111, 97–108 (2021).
17. S.K. Singh, T. Sharan, and A.K. Singh, A comparative performance analysis of various shapes and substrate materials loaded coplanar waveguide-fed antennas. *Mater. Today Proc.* 34, 643–648 (2021).
18. S.K. Singh, T. Sharan, and A.K. Singh, Investigating the S-parameter ( $|S_{11}|$ ) of CPW-fed antenna using four different dielectric substrate materials for RF multiband applications. *AIMS Electron. Electr. Eng.* 6(3), 198–222 (2022).

**Publisher's Note** Springer Nature remains neutral with regard to jurisdictional claims in published maps and institutional affiliations.

Springer Nature or its licensor (e.g. a society or other partner) holds exclusive rights to this article under a publishing agreement with the author(s) or other rightsholder(s); author self-archiving of the accepted manuscript version of this article is solely governed by the terms of such publishing agreement and applicable law.